

**INSTITUTO
DE FÍSICA**

preprint

IFUSP/P-198

**DYNAMICAL COMPONENTS IN THE HEAVY-ION OPTICAL
POTENTIAL⁺**

by

Mahir S. Hussein

**Physics Department, University of Wisconsin-
Madison, Madison, WI 53706 USA**

and

**Instituto de Fisica, Universidade de São Paulo,
C.P.20.516, São Paulo, S.P.**

Brasil*

B.I.F. - USP

**UNIVERSIDADE DE SÃO PAULO
INSTITUTO DE FÍSICA
Caixa Postal - 20.516
Cidade Universitária
São Paulo - BRASIL**

**IFUSP/P 198
B.I.F. - USP**

March, 1980

DYNAMICAL COMPONENTS IN THE HEAVY-ION OPTICAL POTENTIAL[†]

Mahir S. Hussein

Physics Department, University of Wisconsin-Madison, Madison, WI 53706 USA

and

Instituto de Fisica, Universidade de Sao Paulo, CP-20.516

Sao Paulo, S.P. Brazil*

ABSTRACT

Dynamical components in the heavy-ion optical potential are calculated. Special emphasis is given to the dynamical components resulting from coupling to inelastic channels at sub-barrier energies. The component arising from both Coulomb and nuclear coupling is calculated to lowest order using the on-energy-shell approximation for the channel Green's function. A similar approximation is used to calculate the dynamical components arising from particle transfer coupling.

Talk delivered at the Third Oaxtepec Meeting on Nuclear Physics, Oaxtepec, Mexico, January, 1980.

[†]Supported in part by the Tinker Foundation, the U.S.-NSF, the CNPq-Brazil, and FAPESP-Brazil.

*Permanent address

I. Introduction

Most investigations of heavy-ion optical potentials have concentrated on calculating the real part of the potential.¹⁾ Microscopic theories based on the folding model²⁾ as well as macroscopic theories, e.g., the proximity model, have been developed and extensively discussed in the last few years. Recently there has been an upsurge of interest in calculating the imaginary part of the optical potential based on simple physical models. This interest stems from the general recognition of the importance of considering, explicitly, the possible strong coupling of the elastic channel to several reaction channels. Generally, the components in the optical potential arising from the coupling to a specific channel are complex and we shall call these dynamical components. In contrast, we shall call the real part derived from the folding model and the imaginary part that simulates strong absorption static components.

In this paper we present a short review of some of the recent attempts to calculate the dynamical components in the heavy-ion optical potential. In view of the special importance of the sub-barrier coupling to low-lying collective states in modifying the heavy-ion elastic scattering we shall devote a major part of the present review to calculating what has become known as the dynamic polarization potential. This we do in Section II where we shall present two methods: one, the Feshbach reduction procedure, starts with the full coupled channels equations; the other, the semiclassical inverse scattering procedure, is based on Feynman's path integral method. In Section III we discuss the inclusion of nuclear excitation into the dynamical polarization potential. The dynamical component in the optical potential

arising from the coupling to a transfer channel is then discussed and derived in Section IV. Finally, in Section V we give several concluding remarks.

II. Dynamic Components in the Optical Potential

Due to Inelastic Coupling

Recently, Love et al.³⁾ and Baltz et al.⁴⁾ have applied the Feshbach formalism to the calculation of the absorptive potential in the elastic channel for the case of Coulomb excitation. In their calculation the potential was expanded in a perturbation series which was carried out to the lowest non-trivial term. This implies that only the coupling to the first excited state is considered, and thus multiple-step processes, such as those taking place in multiple Coulomb excitation, were not included in the calculation. It is, however, well-known that multiple Coulomb excitation is frequently important in heavy-ion collisions. It is therefore necessary to consider all higher order terms in the perturbation series within some manageable approximation. We should say at the outset that our interest in the dynamic polarization potential, which simulates multiple Coulomb excitation effects on the elastic channel, is not so much in obtaining the correct sub-barrier elastic cross section but rather in its possible use to generate distorted waves which can be then utilized to calculate amplitudes for quasi-elastic processes involving strongly deformed nuclei.

In this section we shall present two methods for calculating the Coulomb polarization potential. The first one is based on the Feshbach reduction procedure referred to above. The second is a semiclassical inversion procedure based on Feynman's path integral method.

A. Feshbach's Reduction Method

In this method one starts with a set of coupled channels equations describing multiple Coulomb excitation⁵⁾ and eliminates all channels in favor of the elastic one. The resulting effective equation describing the system in the elastic channel contains an effective, nonlocal complex energy-dependent orbital angular momentum-dependent potential describing the effect of the eliminated channels on the elastic channel. One then proceeds to construct trivially-equivalent local potentials.³⁾ From the formal point of view the above prescription is easy to realize. However, for the purpose of obtaining closed expressions for the dynamic polarization potential, one needs to resort to several approximations. In refs. 6 and 7 the Feshbach reduction method was utilized to obtain the polarization potential within the approximation of replacing the channel Green's functions by their on-energy-shell (separable) forms. We shall not repeat the steps that lead to the derivation of the potential but refer the reader to refs. 6 and 7 for details. Here we give the final results for the Coulomb polarization potential (CPP) calculated without nuclear excitation. Assuming a quadrupole character for the excited states in the target nucleus we obtain for the CPP:

$$V_{\ell}(r) = -i \frac{\hbar^2}{2\mu} (F(\ell; r))_{02} [1 + iC(\ell)]_{22}^{-1} C_{20}(\ell) \quad (1)$$

where $F(ir)$ is a three-component vector given by

$$(F(\ell; r))_{02} = \left[\begin{array}{l} \frac{F_{\ell_0+2}(k_2 r)}{F_{\ell_0}(k_0 r) r^3} a_{\ell_0 0, \ell_0+2, 2} + \frac{F_{\ell_0}(k_2 r)}{F_{\ell_0}(k_0 r) r^3} a_{\ell_0 0, \ell_0, 2} \\ \frac{F_{\ell_0-2}(k_2 r)}{F_{\ell_0}(k_0 r) r^3} a_{\ell_0 0, \ell_0-2, 2} \end{array} \right] \quad (2)$$

with $F_\ell(k, r)$ being the regular Coulomb wave function in channel j (whose orbital angular momentum is given by $-\vec{I} + \vec{\ell}_0$ with I being the intrinsic spin and $\vec{\ell}_0$ referring to the orbital angular momentum in the entrance channel, which we take to be the ground state). The asymptotic wave number is denoted by k . The matrices $a_{\ell I, \ell' I'}$ enter in the definition of the coupling matrices C via

$$C_{\ell I, \ell' I'} = \frac{1}{k_I} a_{\ell I, \ell' I'} I_{\ell, \ell'}(k_I, k_I) \quad (3)$$

where $I_{\ell, \ell'}(k_I, k_I)$ are the usual Coulomb excitation integrals.⁵⁾ The explicit form of $a_{\ell I, \ell' I'}$ is

$$a_{\ell I, \ell' I'} = \sqrt{a_I a_{I'} \eta_I \eta_{I'}} q_{I \rightarrow I'} \begin{pmatrix} I & I' & 2 \\ 0 & 0 & 0 \end{pmatrix} \frac{1}{\sqrt{(2I+1)(2I'+1)} \sqrt{(2\ell+1)(2\ell'+1)}} \quad (4)$$

$$(-1)^{\ell_0 + I'} \begin{pmatrix} \ell & \ell' & 2 \\ 0 & 0 & 0 \end{pmatrix} \begin{Bmatrix} \ell_0 & \ell' & I' \\ 2 & 1 & \ell \end{Bmatrix}$$

where a_I is half the distance of closed approach for head-on collision in channel I , $a_I = \frac{Z_1 Z_2 e^2}{2(E - E_I)}$, $\eta_I = \frac{Z_1 Z_2 e^2}{\hbar v_I} = k_I a_I$ is the Sommerfeld parameter in channel I (with $Z_i e$ being the charge of nucleus i and v_I the asymptotic velocity in channel I) and $q_{I \rightarrow I'}$ is the symmetrized dimensionless quadrupole strength parameter for the coupling $I \rightarrow I'$ which is defined by

$$q_{I \rightarrow I'} = \frac{\sqrt{\pi}}{5} \frac{\sqrt{\eta_I \eta_{I'}}}{a_I a_{I'}} \frac{\langle I || M(E2) || I' \rangle}{Z_2 e} \times \frac{1}{\sqrt{(2I+1)(2I'+1)} \begin{pmatrix} I & I' & 2 \\ 0 & 0 & 0 \end{pmatrix}} \quad (5)$$

In the limit of a pure quadrupole rotational band and zero energy loss is the different excitation processes we have

$$q_{I \rightarrow I'} = (-1)^{\frac{I+I'+2}{2}} q_{0 \rightarrow 2} \quad (6)$$

The matrix propagator $[1+i\underline{C}]_{22}^{-1}$ has the following structure

$$[1+i\underline{C}(\ell)]_{22}^{-1} = [1+i\underline{C}_{22}(\ell) + \underline{C}_{24}(\ell) [1+i\underline{C}(\ell)]_{44}^{-1} \underline{C}_{42}(\ell)]^{-1}$$

where $[1+i\underline{C}(\ell)]_{44}^{-1}$ is the matrix propagator associated with the 4^+ channel and contains all C's pertaining to $I \geq 4$.

In order to obtain closed expressions for $V_\ell(r)$, we invoke the usual semiclassical approximation

$$I_{\ell\ell}(k_I, k_{I'}) \approx I_{\ell\ell}(k_I, k_{I'}) \sqrt{g_{I \rightarrow I'}(\xi_{I \rightarrow I'})} \quad (7)$$

where the $g_{I \rightarrow I'}$'s are the semiclassical energy loss factors⁸⁾ and $\xi_{I \rightarrow I'}$ is the adiabaticity parameter defined through

$$\xi_{I \rightarrow I'} = \eta_{I'} - \eta_I \approx \frac{\eta_0}{2} \frac{E_{I'} - E_I}{E} \quad (8)$$

E_I is the intrinsic excitation energy of state I. With the use of the usual recursion formulae that connect the Coulomb functions, we were able to cast our potential Eq. (1) in the simple form

$$V_\ell(r) = -i \left(\frac{a_\ell}{r^3} + \frac{b_\ell}{r^4} + \frac{c_\ell}{r^5} \right) \quad (9)$$

where the complex coefficients a_ℓ , b_ℓ and c_ℓ depend on $q_{I \rightarrow I'}$, $\xi_{I \rightarrow I'}$, the center of mass energy, E , and the orbital angular momentum ℓ . In Figs. 1 and 2 we

we exhibit these coefficients as functions of q and ℓ , respectively. Included in this calculation are states up to $J = 16$. All $q_{I \rightarrow I}$, were set equal to 1. It is clear that the imaginary part of $V_\ell(r)$, determined by $\text{Re } a_\ell$, $\text{Re } B_\ell$ and $\text{Re } C_\ell$, behaves basically like r^{-3} for small values of $\bar{\ell} (\equiv \frac{\ell+1/2}{\eta})$ whereas for large $\bar{\ell}$ it goes as r^{-5} . This fact seems to hold irrespective of the value of q . The real part of $V_\ell(r)$ exhibits similar behavior. Note that the real part vanishes identically when all reorientation matrices $C_{ii}^{(\ell)}$ are set equal to zero. We now consider several limiting cases and approximations for $V_\ell(r)$ which have been considered recently.^{4,6)} When all couplings except C_{20} are set equal to zero, we obtain the potential of Baltz et al.⁴⁾ I.e.,

$$\begin{aligned}
 V_\ell^{(2)}(r) &= -i \frac{\hbar^2}{2\mu} (F(r;\ell))_{02} C_{20}^{(\ell)} \\
 &= -i \frac{2}{5} \frac{E}{\eta} q_{0 \rightarrow 2}^2 g_{0 \rightarrow 2}(\xi_{0 \rightarrow 2}) \left(\frac{a}{r}\right)^3 \left[\frac{3\bar{\ell}^2 + 1}{\bar{\ell}^2 (\bar{\ell}^2 + 1)^2} \right. \\
 &\quad \left. - \frac{1}{\bar{\ell}^3} \arctan \bar{\ell} + \frac{4\bar{\ell}^2}{(\bar{\ell}^2 + 1)^2} \left(\frac{a}{r}\right) + \frac{2\bar{\ell}^2}{(\bar{\ell}^2 + 1)^2} \left(\frac{a}{r}\right)^2 \right] \quad (10)
 \end{aligned}$$

Including the reorientation in the 2^+ to all orders we obtain the potential of ref. 6:

$$\begin{aligned}
 V_\ell^{\text{reor}}(r) &= -i \frac{\hbar^2}{2\mu} (F(r;\ell))_{02} \frac{1}{1 + iC_{22}^{(\ell)}} C_{20}^{(\ell)} \\
 &= \text{Re } V_\ell^{\text{reor}}(r) + i \text{Im } V_\ell^{\text{reor}}(r) \quad (11)
 \end{aligned}$$

$$\text{Im } V_\ell^{(2)\text{Reor}}(r) = \left[1 + \frac{4}{49} q_{2 \rightarrow 2}^2 \left(\frac{1}{\bar{\ell}^4} (1 - \arctan \bar{\ell}/\bar{\ell})^2 + \frac{1}{3} \frac{1}{(\bar{\ell}^2 + 1)^2} \right) \right]^{-1} V_\ell^{(2)}(r)$$

and

$$\begin{aligned} \text{Re } V_{\ell}^{(2)\text{Reor}}(r) = & -\frac{4}{35} \left(\frac{E}{\eta}\right) q_{0+2}^2 q_{2+2} \left(\frac{a}{r}\right)^3 g_{02}(\xi_{0+2}) \times \\ & \left[1 + \frac{4}{49} q_{2+2}^2 \left(\frac{1}{\ell} \left(1 - \frac{\arctan \bar{\ell}}{\bar{\ell}} \right)^2 + \frac{1}{3} \frac{1}{(1+\bar{\ell}^2)^2} \right) \right]^{-1} \times \\ & \times \left[\frac{(1-\arctan \bar{\ell}/\bar{\ell})^2}{\bar{\ell}^4} + 2 \frac{(1-\arctan \bar{\ell}/\bar{\ell})}{\bar{\ell}^2} \left(\frac{\bar{\ell}^2-1}{(\bar{\ell}^2+1)^2} \right) \right. \\ & \quad - \frac{1}{3(\bar{\ell}^2+1)^2} - 8 \frac{(1-\arctan \bar{\ell}/\bar{\ell})}{(\bar{\ell}^2+1)^2} \left(\frac{a}{r}\right) \\ & \quad \left. - 4 \frac{\bar{\ell}^2(1-\arctan \bar{\ell}/\bar{\ell})}{(\bar{\ell}^2+1)^2} \left(\frac{a}{r}\right)^2 \right] \end{aligned}$$

where $V_{\ell}^{(2)}(r)$ is given in Eq. (10). Other closed expressions for $V_{\ell}(r)$ can be worked out easily (see Ref. 7 where the excitation of the 4^+ was added to $V_{\ell}^{\text{reor.}}(r)$).

With the help of $V_{\ell}(r)$ one may easily calculate the elastic cross section using for example the WKB approximation. Due to the smallness of $\text{Re } V_{\ell}(r)$ compared to the dominant-monopole-monopole interaction, one expects that for $E < E_B$, the inclusion of $V_{\ell}(r)$ results in a damping factor multiplying the Rutherford cross section.^{4,6)} In Fig. 3 we show such a calculation of σ/σ_R for the system $^{20}\text{Ne} + \text{Sm}$ at $E_{\text{Lab}} = 70 \text{ Mev}$ using the potential $V_{\ell}^{\text{reor.}}(r)$ of Eq. (11). The overall agreement with the data of ref. 9 is good.

It should be clear that the neglect of off-shell effects is expected to be a reasonable approximation only for the lowest order potential $V_{\ell}^{(2)}(r)$. For our general potential of Eq. (1) these effects are expected to be

important and the need to find a simple way of incorporating them is clear. Attempts in this direction have been made⁷⁾ but further work is needed.

B. The Semiclassical Inversion Method

In this subsection we present an alternative method for the evaluation of $V_\ell(r)$. In refs. 10 and 11 $V_\ell(r)$ was evaluated using a semiclassical inversion procedure based on the Alder-Winther theory of multiple Coulomb excitation. The basic input into such a calculation are the amplitudes for finding the system in the elastic channel in the outgoing and ingoing branches of the average classical trajectory. Before actually elaborating the details we first give a brief account of a theory of $V_\ell(r)$ ¹²⁾ based on the Feynman path integral method which would serve as a foundation for the procedure developed in refs. 9 and 10. Recalling Feynman's expression for a transition amplitude K_{00} for scattering by an optical potential $V(r) + V_0(r)$

$$K_{00}(t_1, t_0) = \int_{t_0}^{t_1} \mathcal{D}\vec{r}(t) \exp\left[\frac{i}{\hbar} S[\vec{r}(t)]\right] \quad (12)$$

where $r(t)$ is a path for the relative coordinate satisfying end point (boundary) conditions appropriate for a scattering problem and the path integral extends over all possible paths satisfying these conditions. The action S is given by

$$S[\vec{r}(t)] = \int \left[\frac{1}{2} \mu \dot{r}^2 - V_0(\vec{r}) - V(\vec{r}) \right] dt \quad (13)$$

where $V_0(r)$ is some already known potential (e.g., for sub-barrier energies $V_0(r)$ is the monopole-monopole Coulomb potential). For $V(r)$ to represent correctly the effect on the elastic channel due to its coupling to other

channels it must be such as to give for K identical results as those obtained from a microscopic description of the reaction. Now we assume that the intrinsic motion of the fragments as described by a Hamiltonian H_0 with eigenstates $\{|i\rangle\}$ and energies $\{\epsilon_i\}$. The time evolution operator U of the interacting system obeys the usual equation

$$i\hbar \frac{\partial}{\partial t} U = [H_0 + V(\vec{r}(t), \xi)]U \quad (14)$$

where $V(\vec{r}(t), \xi)$ is a potential which represents the coupling between the relative motion, described by $\vec{r}(t)$ and the internal (intrinsic) coordinates $\{\xi\}$. Equation (14) is to be solved with the boundary condition $U = 1$ at $t = t_0$ for a given path $\vec{r}(t)$. The amplitude K_{00} for the system to remain in the ground state at time t_1 is then given by¹²⁾

$$K_{00}(t_1, t_0) = \int_{t_0}^{t_1} \mathcal{D}\vec{r}(t) \exp\left[\frac{i}{\hbar} S_0(\vec{r}(t))\right] \langle 0|U(\vec{r}, t_1, t_0)|0\rangle \quad (15)$$

where the free action $S_0(\vec{r}(t))$ is given by

$$S_0(\vec{r}(t)) = \int_{t_0}^{t_1} \left[\frac{1}{2} m \dot{\vec{r}}^2 - V_0(\vec{r}) \right] dt \quad (16)$$

It is then clear that $K_{00}(t_1, t_0)$ of Eq. (15) and that of Eq. (12) are identical if we have

$$\langle 0|U(\vec{r}, t_1, t_0)|0\rangle = \exp\left[-\frac{i}{\hbar} \int_{t_0}^{t_1} V(\vec{r}(t)) dt\right] \quad (17)$$

for all paths $\vec{r}(t)$ connecting t_0 and t_1 . In particular, if we are to use a semiclassical approximation in the evaluation of (12) and (15), which is

a reasonable procedure for heavy ion scattering, then Eq. (17) is still valid with \vec{r} replaced by the real classical trajectory $\vec{r}_{cl}(t)$ that satisfies the classical equation of motion

$$\mu \ddot{\vec{r}}_{cl} + \vec{\nabla} \text{Re } V(\vec{r}_{cl}) + \vec{\nabla} \text{Re } V_o(\vec{r}_{cl}) = 0 \quad (18)$$

or

$$\mu \ddot{\vec{r}}_{cl} - \hbar \vec{\nabla} \text{Im } \ln \langle 0 | U(\vec{r}_{cl}, t_1, t_0) | 0 \rangle + \vec{\nabla} \text{Re } V_o(\vec{r}_{cl}) = 0 \quad (19)$$

The above relations give a prescription for calculating the classical force resulting from the coupling between the relative and the intrinsic motions. For simple applications of the above methods, we restrict ourselves to real trajectories only. The most straightforward application of Eq. (17) is for the case where $t_0 = -\infty$ and $t_1 = +\infty$; i.e., in the asymptotic region. This, however, will give us the potential in the asymptotic region and there is no reason to expect that the resulting potential, when inserted back into Eq. (12), will generate the amplitude K_{oo} at any time t_1 . In order to compare the potential derived according to the semiclassical prescription with that of the previous subsection, we have to extract from K_{oo} of Eq. (17) a potential which, when inserted into Eq. (12), would generate the same K_{oo} at any time t_1 (or separation between the two ions). Furthermore, we believe that such wave-function equivalent potentials are required to generate the correct distorted waves which enter in the evaluation of DWBA amplitudes describing quasielastic processes occurring in the collision between deformed nuclei.

Our prescription for the calculation of the wave function equivalent optical potential rests on several observations:

a) Calculate the average classical trajectory $\vec{r}_\ell(t)$. Although this requires the knowledge of $\langle 0|U|0\rangle$, we shall, in the following, assume that $\vec{r}_\ell(t)$ is given by the Rutherford trajectory which is a reasonable approximation for the energies ($E < E_B$) and the systems ($\eta \gg 1$, $\xi \ll 1$) considered.

b) Evaluate the impact parameter-dependent $V(r)$ (implicit in our considerations) at a given radial separation distance r from Eq. (17), both in the ingoing ($V_\ell^{(-)}(r)$) and outgoing ($V_\ell^{(+)}(r)$) branches of the Rutherford trajectory (see Fig. 4).

c) Calculate the wave-function equivalent potential from the algebraic mean of $V_\ell^{(+)}(r)$ and $V_\ell^{(-)}(r)$; i.e.,

$$V_\ell(r) = \frac{1}{2} (V_\ell^{(-)}(r) + V_\ell^{(+)}(r)) \quad (20)$$

The justification for the prescription in (20) is given in refs. (10) and (11) and it basically resides in the insistence that $V_\ell(r)$ as calculated above should be the same (or at least equivalent to) the trivially equivalent local potential derived in subsection IIa.

Clearly in order to carry out the evaluation of $V_\ell(r)$ according to Eq. (20), one needs to know the amplitudes $a_\ell^{(-)}(t)$ and $a_\ell^{(+)}(t)$ for finding the system in the elastic channel at time t (or separation r) on the ingoing and outgoing branches of the Rutherford trajectory respectively (these are just the amplitudes $\langle 0|U^{(-)}|0\rangle$ and $\langle 0|U^{(+)}|0\rangle$). For pure multiple Coulomb excitation the de Boer-Winther code does supply these amplitudes and one could, therefore, evaluate $V_\ell(r)$ numerically if needed. However, in order to study the properties of $V_\ell(r)$, we consider instead the closed expressions for $a_\ell^{(-)}$ and $a_\ell^{(+)}$ valid in the sudden limit given by Alder-Winther⁵⁾ (for pure quadrupole coupling). These amplitudes are given by:

$$a_{\ell}^{(\pm)} = \frac{1}{4\pi} \int_0^{2\pi} d\alpha \int_0^{\pi} \sin\beta d\beta \exp\left[-i \frac{4E\eta^2}{v} q \int_{-\infty}^{t_{\ell}^{\pm}(r)} dt \frac{P_2(\cos x^{\pm}(t))}{r_{\ell}^3(t)}\right] \quad (21)$$

where α, β are the Euler angles that specify the orientation of the target symmetry axis, η the Sommerfeld parameter given by $\frac{Z_1 Z_2 e^2}{\hbar v}$, P_2 is the Legendre polynomial of order two and $\chi^{\pm}(t)$ are the angles subtended by the target symmetry axis and the line connecting the centers of the two nuclei; i.e., $\cos x^{\pm}(t) = \cos\beta \cos\theta_{\ell}^{\pm}(t) + \sin\beta \sin\theta_{\ell}^{\pm}(t) \cos(\alpha - \phi_{\ell}^{\pm}(t))$, where $\theta_{\ell}^{\pm}(t)$ and $\phi_{\ell}^{\pm}(t)$ are the spherical polar angles that determine the orientation of the line joining the centers of the colliding nuclei. The times $t_{\ell}^{-}(r)$ and $t_{\ell}^{+}(r)$ are those at which the distance between centers is r for the ingoing (-) and outgoing (+) branches of the trajectory, respectively. Using the above form of the amplitudes $a_{\ell}^{(-)}(r)$ and $a_{\ell}^{+}(r)$, we can now write down our final expression for $V_{\ell}(r)$

$$V_{\ell}(r) = -\frac{\hbar^2 \ell}{2\mu r^2} \left\{ \frac{\langle e^{-iE^{+}}(r) \frac{dE^{+}(r)}{d\theta} \rangle}{\langle e^{-iE^{+}}(r) \rangle} - \frac{\langle e^{-iE^{-}}(r) \frac{dE^{-}(r)}{d\theta} \rangle}{\langle e^{-iE^{-}}(r) \rangle} \right\} \quad (22)$$

where $\langle \rangle$ refers to $\int_0^{2\pi} d\alpha \int_0^{\pi} \sin\beta d\beta$ and

$$E^{(\pm)}(r) = A_1^{\pm}(r) \cos^2 \beta + A_2^{\pm}(r) \sin 2\beta \cos \alpha + A_3^{\pm}(r) \sin^2 \beta \cos^2 \alpha - A_4^{\pm}(r) \quad (23)$$

Here

$$\begin{aligned} A_1^{\pm}(r) &= \pm A_1^0(\pm\theta_0) \mp A_1^0(\theta) \\ A_2^{\pm}(r) &= \pm A_2^0(\pm\theta_0) \mp A_2^0(\theta) \\ A_3^{\pm}(r) &= \pm A_3^0(\pm\theta_0) \mp A_3^0(\theta) \\ A_4^{\pm}(r) &= \pm A_4^0(\pm\theta_0) \mp A_4^0(\theta) \end{aligned} \quad (24)$$

where the elementary trajectory integrals $A_i^0(\theta)$ are given by

$$A_1^0(\theta(r)) = 3q_{0 \rightarrow 2} \left(\frac{\mu v a}{\hbar \ell}\right) \left(\frac{\eta}{\ell}\right)^2 \left[\sqrt{\frac{\ell^2}{\eta^2} + 1} \left(\sin\theta - \frac{\sin^3\theta}{3} \right) - \frac{\sin 2\theta}{4} - \frac{\theta}{2} \right] \quad (25)$$

$$A_2^0(\theta(r)) = 3q_{0 \rightarrow 2} \left(\frac{\mu v a}{\hbar \ell}\right) \left(\frac{\eta}{\ell}\right)^2 \left[\sqrt{\frac{\ell^2}{\eta^2} + 1} \left(\frac{1 - \cos^3\theta}{3} \right) - \frac{\sin^2\theta}{2} \right] \quad (26)$$

$$A_3^0(\theta(r)) = 3q_{0 \rightarrow 2} \left(\frac{\mu v a}{\hbar \ell}\right) \left(\frac{\eta}{\ell}\right)^2 \left[\sqrt{\frac{\ell^2}{\eta^2} + 1} \left(\frac{\sin^3\theta}{3} - \frac{\theta}{2} + \frac{\sin 2\theta}{4} \right) \right] \quad (27)$$

and

$$A_4^0(\theta(r)) = q_{0 \rightarrow 2} \left(\frac{\mu v a}{\hbar \ell}\right) \left(\frac{\eta}{\ell}\right)^2 \left[\sqrt{\frac{\ell^2}{\eta^2} + 1} \sin\theta - \theta \right] \quad (28)$$

In the above θ is related to r through the trajectory equation

$$\left(\frac{a}{r}\right) = \left(\frac{\eta}{\ell}\right)^2 \left[\sqrt{\left(\frac{\ell}{\eta}\right)^2 + 1} \cos\theta - 1 \right] \quad (29)$$

Finally θ_0 is the asymptotic value of θ ; i.e.,

$$\tan\theta_0 = \frac{\ell}{\eta} \quad (30)$$

One immediate result we obtain is the potential $V_\ell(r)$ of Eq. (22) calculated to second order in $q_{0 \rightarrow 2}$. Expanding the exponentials and using the explicit forms of the $A_i^\pm(\theta)$'s, it is easy to verify that the resulting potential coincides exactly with $V_\ell^{(2)}(r)$ of Eq. (10) of the last subsection. This gives us more confidence in our semiclassical theory of $V_\ell(r)$ summarized in Eqs. (17) and (20). For large values of the coupling $q_{0 \rightarrow 2}$, Eq. (22) has to be solved numerically and the results of this calculation are

summarized in Fig. 5, where we have plotted $(\frac{r}{a})^3 \frac{\eta}{E} V_\ell(r) \equiv W_\ell(q)$ as a function of $q_{0 \rightarrow 2}$ and have set $r = r_t(\ell)$, the ℓ -dependent classical turning point. Both the real and imaginary parts of $W_\ell(q)$ exhibit oscillatory behaviors as functions of $q_{0 \rightarrow 2}$. This behavior is clearly a consequence of multiple Coulomb excitation effects. This behavior is not shared by the potential calculated in subsection IIa indicating the importance of the off-shell terms which were completely neglected and which are presumably indirectly present in the semiclassical potential. The dashed-dotted curve in Fig. 5 is the $\ell = 0$ component of a potential calculated directly from the asymptotic amplitude; i.e., from $a_\ell^{(+)}(r=\infty)$ (notice that $a_\ell^{(-)}(r=\infty) = 0$).

This phase-shift equivalent potential, which we call $V_\ell^{\text{AW}}(r)$ (AW = Alder-Winther), exhibits quite a different behavior from our semiclassical $V_\ell(r)$ of Eq. (22). In ref. 11 a detailed discussion of this difference was given in connection with a recent numerical calculation¹⁴⁾ of $V_\ell^{\text{AW}}(r)$ which uses an inverse scattering method whose input are the asymptotic phase shifts extracted from the de Boer-Winther code. Finally, it is important to realize that although the imaginary part of our potential $V_\ell(r)$ for a given value of ℓ becomes positive at several values of q , and thus violating the condition of absorption for that particular partial wave, for other values of ℓ the imaginary part at those q 's referred to above is negative and it is clear that the overall effect of $V_\ell(r)$ is absorptive by construction. Notice also that the potentials shown in Fig. 5 were evaluated at the classical turning point $V_t(\ell)$ and their values and signs at a given q clearly change as the radial separation increases. To check this we have evaluated $\text{IM } V_{\ell=0}(r)$ for $q_{0 \rightarrow 2} = 7$ and found that it is positive only at, and only slightly outside of, the classical turning point $r = 2a$. For larger values of r ,

$\text{Im } V_\ell(r)$ is negative. This behavior also holds for other values of ℓ . Since Fig. 5 refers to $V_\ell(r)$ calculated assuming a pure rotational character of the excited states in the target, it is therefore of interest to find the $V_\ell(r)$ in the case of pure vibrational states. Such a calculation was made in ref. 15 and the surprising result was that if the assumption of a pure harmonic quadrupole vibration is made for the excited states in the target, then the resulting potential, calculated in the sudden limit according to Eq. (20), is the same as $V_\ell^{(2)}(r)$ of Eq. (10)! The fact that the potential comes out to be pure imaginary in this case is expected since for vibrational states $C_{ii}(\ell)$ of Eq. (1) are zero. The difference between $V_\ell^{(2)}(r)$ and $V_\ell(r)$ of Fig. 5 must therefore be due to, among other things, the phonon-phonon interactions (anharmonic terms) which are very important for rotational nuclei.

III. The Dynamic Polarization Potential due to Coulomb and Nuclear Couplings

In Section II we derived expressions for the Coulomb polarization potential assuming only Coulomb coupling of the elastic channel to the different inelastic channels. Therefore the potential $V_\ell(r)$ of Eqs. (20) and (22) is appropriate in the description of elastic scattering at sub-barrier energies. At energies above the barrier, the nuclear coupling becomes important and therefore one needs to modify the expression for $V_\ell(r)$. Besides the coupling the static component of the optical potential contains both the repulsive monopole-monopole Coulomb interaction and the attractive nuclear potential. We shall, in the following, outline the derivation of an expression for $V_\ell(r)$ to second order in the Coulomb-nuclear coupling using

Feshbach's reduction method (for details see ref. 16). We start from the coupled-channels equations for the radial wave function in the elastic

channel $\chi_{(\ell_0 0)\ell_0}(k, r)$

$$\left[\frac{d^2}{dr^2} + k_n^2 - \frac{\ell_n(\ell_n+1)}{r^2} - \frac{2\mu_n}{\hbar^2} V_0(r) \right] \chi_{(\ell_n I_n)J}(k_n, r) e^{i\sigma_{\ell_n}(k_n)} \quad (31)$$

$$= \sum_{\ell_m I_m} \frac{2\mu_n}{\hbar^2} V_{\ell_n I_n, \ell_m I_m}^J(r) \chi_{(\ell_m I_m)J}(k_m, r) e^{i\sigma_{\ell_m}(k_m)},$$

where μ is the reduced mass and $\sigma_{\ell}(k_I)$ is the Rutherford phase shift in channel I. We write the coupling interaction as

$$V_{\ell_0 0, \ell I}(r) = a_{\ell_0 \ell} F_L(r) \quad (32)$$

where $F_L(r)$ is the form factor for the inelastic transition with multipolarity L and $a_{\ell_0 \ell}$ contains geometrical factors. Using the methods developed in ref. 17, we obtain for $V_{\ell}^{(2)}(r)$ the following

$$V_{\ell}^{(2)}(r) = -i \frac{\mu_n k}{2\pi \hbar^2} F_L(r) \sum_{K=-L}^L [a_K(\ell)]^2 T_{LK}(\ell) f_K(\ell, r). \quad (33)$$

where $K = \ell_0 - \ell$ and we have written $a_{\ell_0 \ell} \equiv a_K(\ell)$. The quantities $T_{LK}(\ell)$ are given by

$$T_{LK}(\ell) = \frac{R_{\ell' \ell}^L(k', k)}{[S_{\ell'}^{(N)}(k') S_{\ell}^{(N)}(k)]^{1/2}}, \quad (34)$$

where

$$R_{\ell' \ell}^L(k', k) = \frac{4\pi}{k' k} \int_0^{\infty} dr \chi_{\ell'}^0(k', r) F_L(r) \chi_{\ell}^0(k, r) \quad (35)$$

are the radial integrals for the form factors $F_L(r)$ between the distorted waves $\chi_\ell^{\circ}(r)$ pertaining to the static component of the optical potential $V_0(r)$, and $S_\ell^{\circ(N)}(k)$ are the nuclear parts of the partial-wave ℓ -matrix elements for elastic scattering by $V_0(r)$. Finally the functions $f_K(\ell, r)$ are given by

$$f_K(\ell, r) = \frac{F_{\ell-K}(k'r)}{F_\ell(kr)}, \quad (36)$$

where $F_\ell(kr)$ are the regular Coulomb wave functions. Considering the case of quadrupole excitation, $L = 2$, and using the following approximation for $f_K(\ell, r)$

$$f_2(\ell, r) \sim f_{-2}(\ell, r) \approx -1 + \frac{2}{\lambda^2 + \bar{\eta}^2} \left(\bar{\eta}^2 + \frac{2\bar{\eta}\lambda^2}{kr} + \frac{\lambda^4}{k^2 r^2} \right), \quad (37)$$

where $\lambda \equiv \ell + \frac{1}{2}$ and $k \equiv \frac{k_0 + k_2}{2}$ and $\bar{\eta}$ is the average Sommerfeld parameter.

We obtain after using the explicit form of $a_K(\ell)$ given in Eq. (3) (without the q) and resorting to the approximation used to evaluate $T(\ell)$ given in ref. (17)

$$\begin{aligned} V_\ell^{(2)}(r) \approx & -i \frac{k}{2} F_2(r) \frac{1}{16\pi} \left\{ \left[\delta_2^{(c)} \left(\frac{6}{5} \right) \frac{\eta^2}{\ell^2} \left(1 - \frac{\arctan \frac{\ell}{2}}{\frac{\ell}{\eta}} \right) \left(\frac{R}{a} \right) \right. \right. \\ & \left. \left. - i \delta_2^{(N)} \frac{dS_\ell^{\circ(N)}}{d\ell} [S_\ell^{\circ(N)}(\ell)]^{-1} \right] \right. \\ & + 3 \left[\delta_2^{(c)} \frac{2}{5} \frac{R}{a} \frac{\eta^2}{\ell^2 + \eta^2} - i \delta_2^{(N)} \frac{dS_\ell^{\circ(N)}}{d\ell} [S_\ell^{\circ(N)}(\ell)]^{-1} \right] \left(\frac{4}{\ell^2 + \eta^2} \right) \frac{\eta^2 \ell^2}{k} \frac{1}{r} \\ & + 3 \left[\delta_2^{(c)} \frac{2}{5} \frac{R}{a} \frac{\eta^2}{\ell^2 + \eta^2} - i \delta_2^{(N)} \frac{dS_\ell^{\circ(N)}}{d\ell} [S_\ell^{\circ(N)}(\ell)]^{-1} \right] \left(\frac{2}{\ell^2 + \eta^2} \right) \frac{\eta^2 \ell^2}{k^2} \frac{1}{r^2} \\ & \left. + 3 \left[\delta_2^{(c)} \frac{2}{5} \left(\frac{R}{a} \right) \frac{\eta^2}{\ell^2 + \eta^2} - i \delta_2^{(N)} \frac{dS_\ell^{\circ(N)}}{d\ell} [S_\ell^{\circ(N)}(\ell)]^{-1} \right] \left[-1 + \frac{2\eta^2}{\ell^2 + \eta^2} \right] \right\} \end{aligned} \quad (38)$$

where the approximation of large- λ has been used. In the above $F_2(r)$ is given by

$$F_2(r) = \delta_2^{(C)} \frac{3}{5} Z_1 Z_2 e^2 \frac{R}{r^3} - \delta_2^{(N)} \frac{dV_N(r)}{dr} \quad (39)$$

where $\delta_2^{(C)} = \beta_2^{(C)} R_C$ and similarly for $\delta_2^{(N)}$. In Eq. (38), $\overset{\circ}{S}^{(N)}(\ell)$ is the nuclear part of the elastic S -matrix element corresponding to the scattering by $V_0(r)$. In the limit that the nuclear part of $V_0(r)$ is not felt, then $\overset{\circ}{S}^{(N)}(\ell) = 1$ and $\frac{d\overset{\circ}{S}^{(N)}}{d\ell} = 0$, we recover the second order pure imaginary potential $V^{(2)}(r)$ of Eq. (10). Due to the presence of $\overset{\circ}{S}^{(N)}$, the potential of Eq. (38) is complex. Of course in order to actually use $V(r)$ above in e.g., optical model analysis of elastic scattering, one needs to know $\overset{\circ}{S}^{(N)}(\ell)$. This can either be made through the evaluation of $\overset{\circ}{S}^{(N)}(\ell)$ by first setting $\delta_2^{(C)} = 0$ and then solving the optical model equation or by using simple parametrized forms.¹⁶⁾

IV. The Dynamical Component Resulting from Transfer Coupling

Turning to rearrangement channels, it should be emphasized that while we are well aware of the non-orthogonality of the initial and final states in these cases, we disregard the contributions from nonvanishing overlap integrals of the internal wave functions on the expectation that these are of lesser importance for heavy than for light projectile.¹⁸⁾ To present the result in the simplest form, we consider, in addition to zero spin nuclei, transfers with $L = 0$ only. Then the form factor for transfer into a bound state of imaginary wave number $K = (2\mu_c E_b)^{1/2}/\hbar$ where μ_c is the reduced mass and E_b the binding energy of the transferred particle, is

$$F_0^{(K)}(r) = \frac{e^{-Kr}}{Kr} \quad (40)$$

Now the effective transfer coupling potential becomes

$$V_{\ell}^{(T)}(r) = -i \frac{\mu k}{2\pi\kappa^2} a_T^{(\kappa_1)} a_T^{(\kappa_2)} T_{00}^{(\kappa_1)}(\ell) F_0^{(\kappa_2)}(r) f_0(\ell, r), \quad (41)$$

where the constants $a_T^{(\kappa)}$ are proportional to the product of the spectroscopic factors and the zero-range overlap integral μ is the reduced mass in the incident channel, κ_1 and κ_2 are the bound-state wave numbers of particle C before and after the transfer. With the same approximations as in ref. 15 the final expression for $V_{\ell}^{(T)}(r)$ becomes after setting $f_0(\ell, r) \approx 1$ is

$$V_{\ell}^{(T)}(r) = -i \frac{\mu}{\zeta k' \kappa^2} \frac{a_T^{(\kappa_1)}}{\kappa_1} \frac{a_T^{(\kappa_2)}}{\kappa_2} I_{00}^{(\kappa_1)}(\delta, \xi) \frac{e^{-\kappa_2 r}}{r}. \quad (42)$$

where ζ is a scale factor arising from the non-recoil approximation and $I_{00}^{(\kappa)}(\delta, \xi)$ is the WKB approximation to the Coulomb radial integrals for transfer with $\delta = 2 \arctan\left(\frac{\eta}{\lambda + 1/2}\right)$ and ξ is the adiabaticity parameter defined by $\eta_f - \eta_i$. As shown in ref. 16, since $I_{00}^{(\kappa)}(\delta, \xi)$ falls off exponentially ($\exp[-(\frac{\kappa}{k})\ell]$) at large ℓ , the contribution to the S-matrix corresponding to Eq. (42) is localized in ℓ -space. Since the asymptotic form of $I_{00}^{(\kappa)}(\delta, \xi)$ is real, the dynamical component (42) is predominantly absorptive.

In reactions where the single transfer of a cluster c leads into a channel that is identical to the elastic channel (elastic transfer, ET), the effective coupling potential has the form (for $L = 0$)

$$V_{\ell}^{(ET)}(r) = (-)^{\ell} a_T^{(\kappa_1)} F_0^{(\kappa_1)}(r) = (-)^{\ell} \frac{a^{(\kappa_1)}}{\kappa_1} \frac{e^{-\kappa_1 r}}{r}, \quad (43)$$

which is a real exchange potential.

Finally, we consider reactions in which the successive transfer of a cluster c leads back into the elastic channel. Then the contribution to the effective potential corresponding to the two diagrams of Fig. 6 becomes

$$V_{\lambda}^{(DT)}(r) = [1 + (-)^{\lambda}] V_{\lambda}^{(T)}(r) \quad (44)$$

with $V_{\lambda}^{(T)}(r)$ given by Eq. (42). The potential $V_{\lambda}^{(DT)}(r)$ exhibits clearly even-odd staggering effects.

V. Conclusion

In this paper we have derived expressions for the different dynamical components in the heavy-ion optical potentials. For sub-barrier elastic scattering the Coulomb polarization potential (CPP) was derived using two different methods; the Feshbach reduction method based on the time independent coupled channels equations, and the semiclassical inversion method based on Feynman's path integral method. We have demonstrated that the two methods give identical results for the CPP if calculated to second order in the quadrupole coupling parameter. In the general case of intermediate or strong coupling, the two methods give different results. This is partly attributed to the neglect of off-shell effects in the Feshbach reduction method.

We have also obtained expressions for the dynamical components due to Coulomb and nuclear coupling to an inelastic 2^+ channel. The potential exhibits the general features connected to the Coulomb-nuclear interference effects. The λ -dependence of the potential shows clearly the presence of

an l -window connected to the nuclear excitation.

Finally the component due to transfer coupling was obtained within the on-energy-shell approximation, for the $L = 0$ case. The expression found has a very simple r - and l -dependence which would result in a well-defined l -window in the corresponding elastic S -matrix element.

Acknowledgements

Several people have collaborated with me on different aspects of the questions discussed in this paper. These are: B. V. Carlson, L. F. Canto, R. Donangelo, W. E. Frahn, A. J. Baltz and M. P. Pato.

REFERENCES

1. For a review see, R.G. Satchler and W. G. Love, Phys. Rep. 55 (1979) 183.
2. D. M. Brink and Fl. Stanku, Nucl. Phys. A 299 (1978) 23.
3. W. G. Love et al., Phys. Rev. Lett. 39 (1977) 6.
4. A. J. Baltz et al. 40 (1978) 20.
5. K. Alder and Aa. Winther, Electromagnetic Excitation (North Holland 1975).
6. M. S. Hussein, Phys. Lett. B, in press.
7. B. V. Carlson, M.S. Hussein and A.J. Baltz, in preparation; B.V. Carlson and M. S. Hussein, in preparation.
8. K. Alder, A. Bohr, T. Huus, B. Mottelson and Aa. Winther, Rev. Mod. Phys. 28 (1958) 1432.
9. P. Doll et al., Phys. Lett. 76B (1978) 566.
10. R. Donangelo, L.F. Canto and M.S. Hussein, Nucl. Phys. A320 (1979) 422.
11. M. S. Hussein, M.P. Pato, L.F. Canto and R. Donangelo, submitted for publication.
12. D. M. Brink, private communications; K. Mohring and U. Smilansky, Berlin preprint (1979)
13. P. Pechukas, Phys. Rev. 181 (1969) 174.
14. P. Frobrich, R. Lipperheide and H. Fiedeldey, Phys. Rev. Lett. 43 (1979) 1147.
15. R. Donangelo, L.F. Canto and M.S. Hussein, Phys. Rev. C19 (1979) 1801.
16. W. E. Frahn and M.S. Hussein, to be published.
17. W. E. Frahn and M.S. Hussein, Proceedings of the Symposium on Heavy Ion Physics from 10 to 200 MeV/AMU, Brookhaven National Laboratory, July 16-20 (1979), and to be published.
18. B. Imanishi, M. Ichimura and M. Kawai, Phys. Lett. 52B (1974) 267.

FIGURE CAPTIONS

- Figure 1 The coefficient a_ℓ , b_ℓ and c_ℓ plotted as functions of $\bar{\ell} \equiv \frac{\ell + 1/2}{\eta}$ for several values of the quadrupole coupling parameter q . A factor $\frac{\eta}{E}$ was taken out of the coefficients in order to present the result in as general a form as possible.
- Figure 2 The coefficient, a_ℓ , b_ℓ and c_ℓ plotted as functions of the quadrupole coupling parameter q for several values of $\bar{\ell} \equiv \frac{\ell + 1/2}{\eta}$. A factor $\frac{\eta}{E}$ was taken out of the coefficients (see caption to Fig. 1).
- Figure 3 The sub-barrier elastic cross section normalized to the Rutherford cross section, plotted vs. the center of mass angle for the system $^{20}\text{Ne} + \text{Sm}$ ($E_{\text{lab}} = 70 \text{ MeV}$). Included in the calculation is the coupling to the 2^+ state as well as the re-orientation of the 2^+ to all orders in both target and projectile. The data are from Ref. 9.
- Figure 4 Terms contributing to the semiclassical optical potential: (a) ingoing wave; (b) outgoing wave.
- Figure 5 The Coulomb polarization potential vs. q plotted is $\frac{\eta}{E} \left(\frac{r_t(\ell)}{a} \right)^3 V_\ell(r_t(\ell))$ for $\bar{\ell} (\equiv \frac{\ell}{\eta}) = 0.0, 1.0$ and 2.0 . a) the imaginary part, b) the real part. The dashed-dotted line is the Alder-Winther potential (see text).
- Figure 6 Two-step elastic transfer processes represented by the effective potential $V_\ell^{(DT)}(r)$.

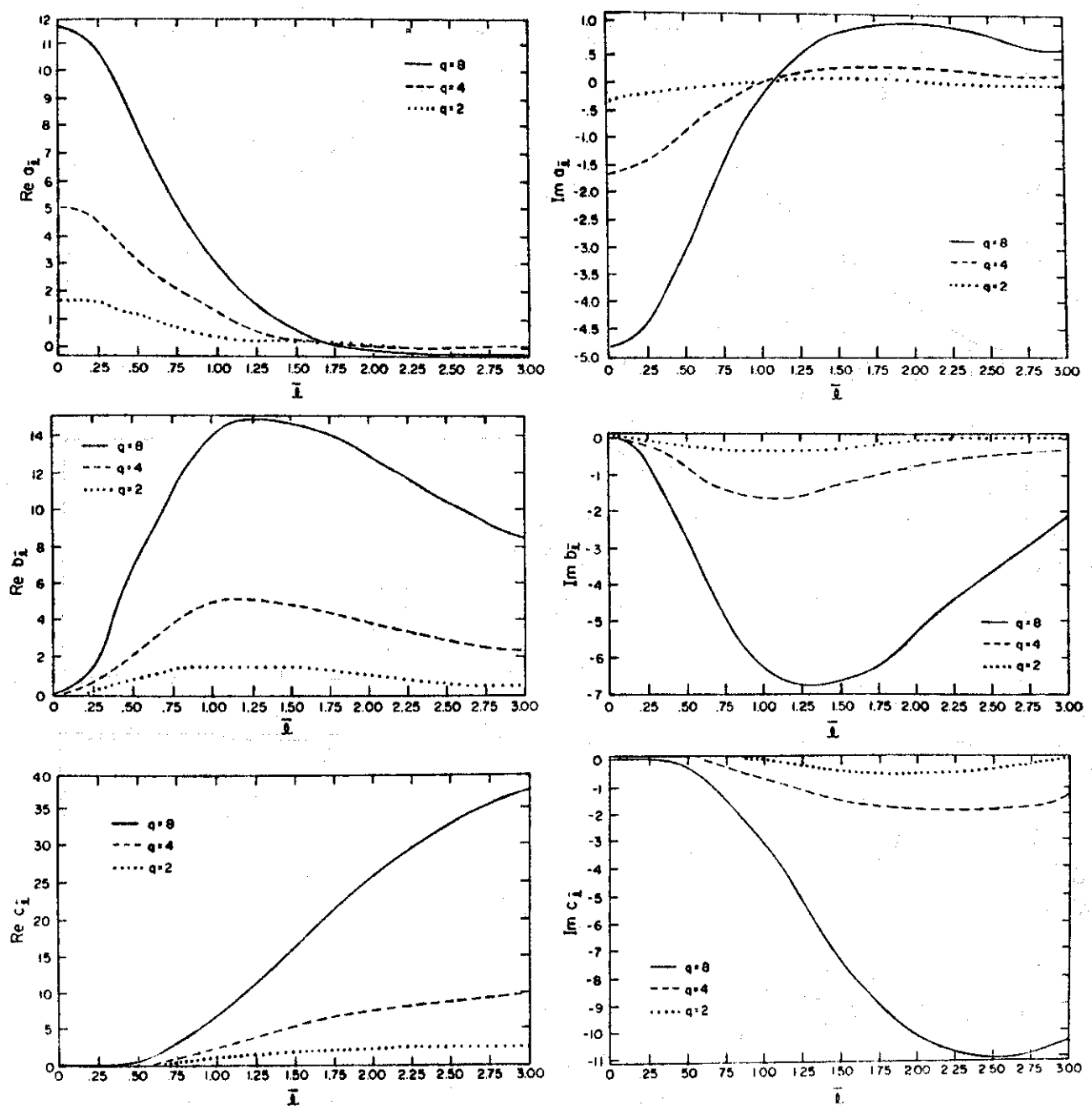


FIG. 1

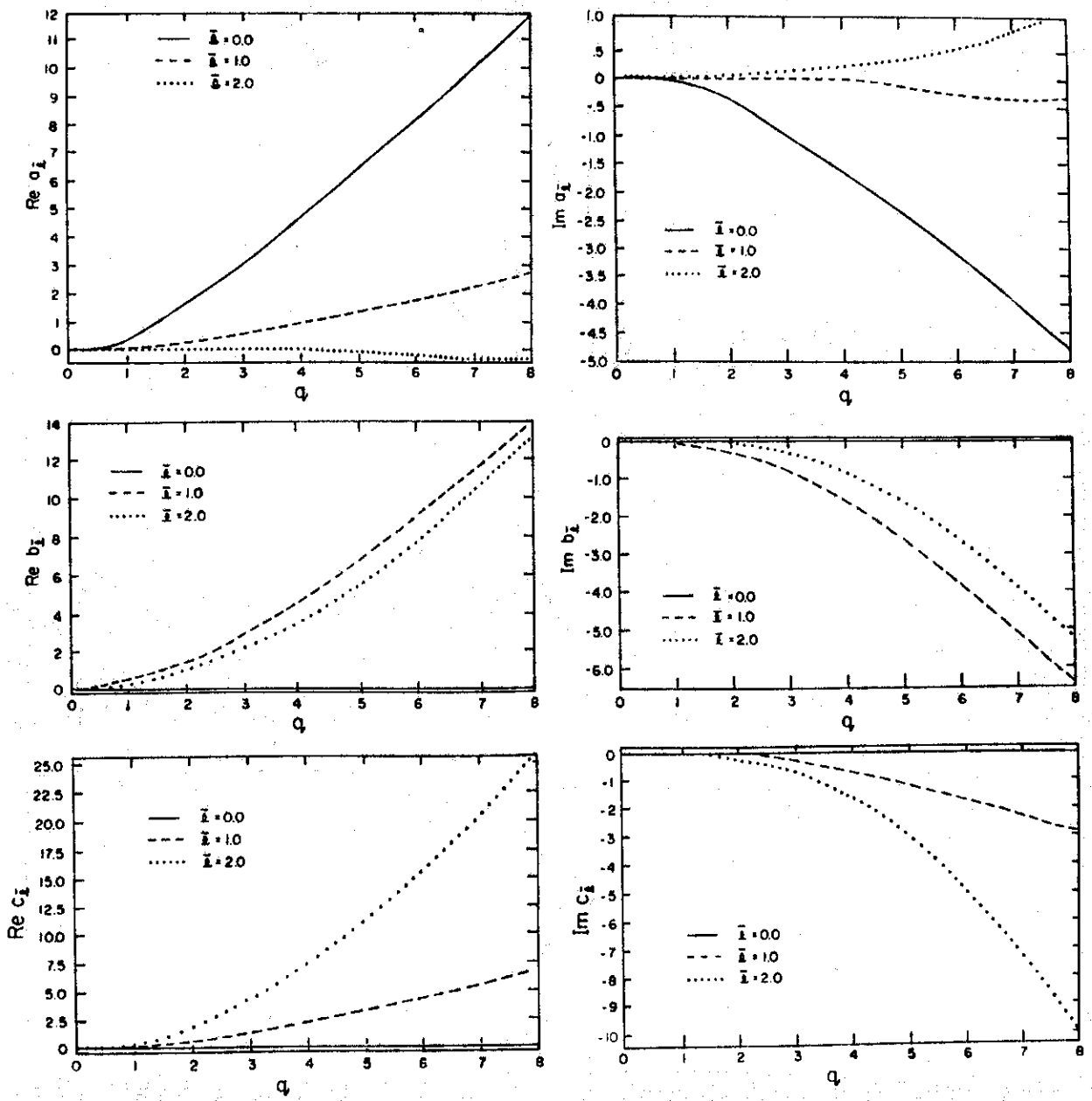


FIG. 2

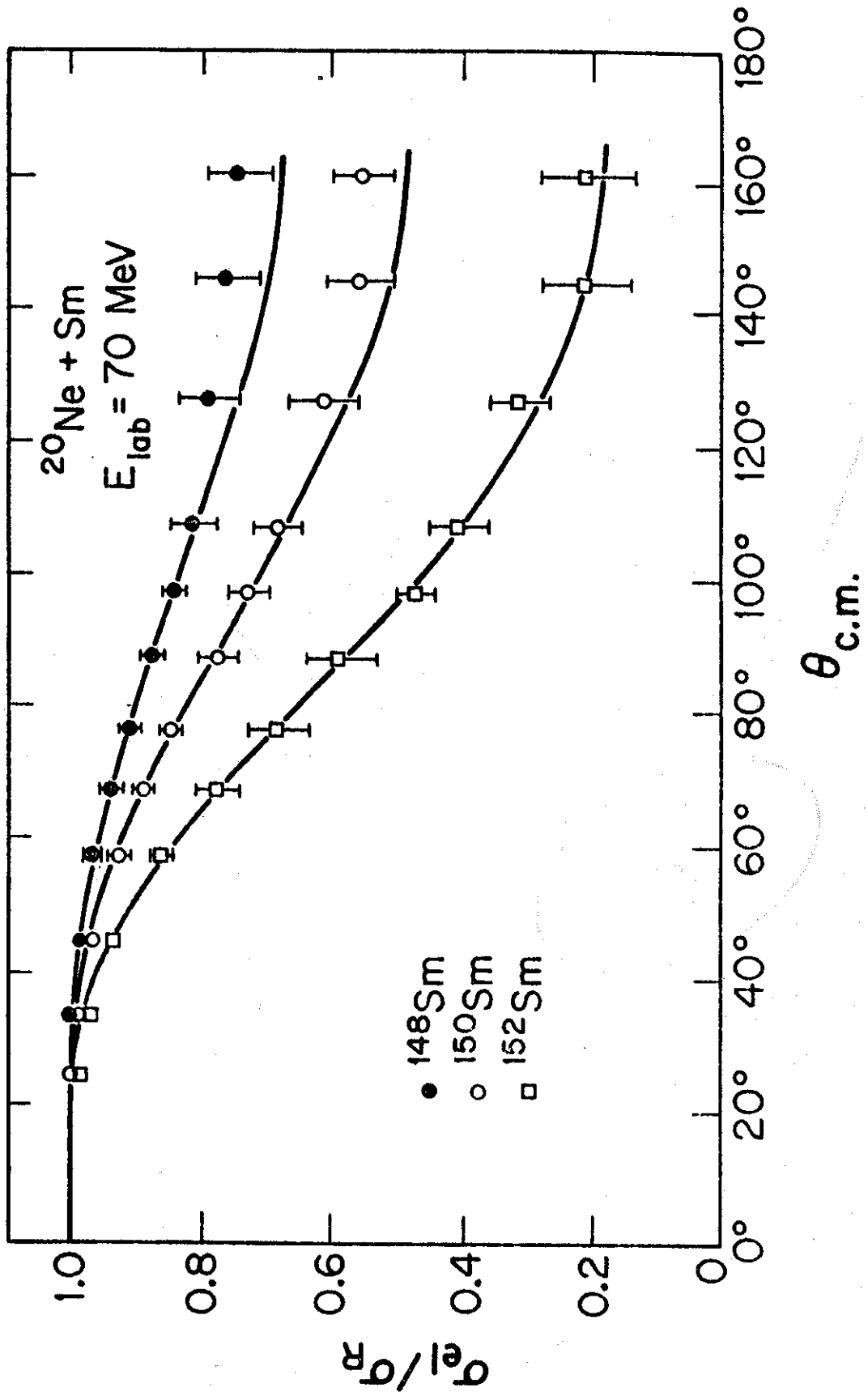


FIG. 3

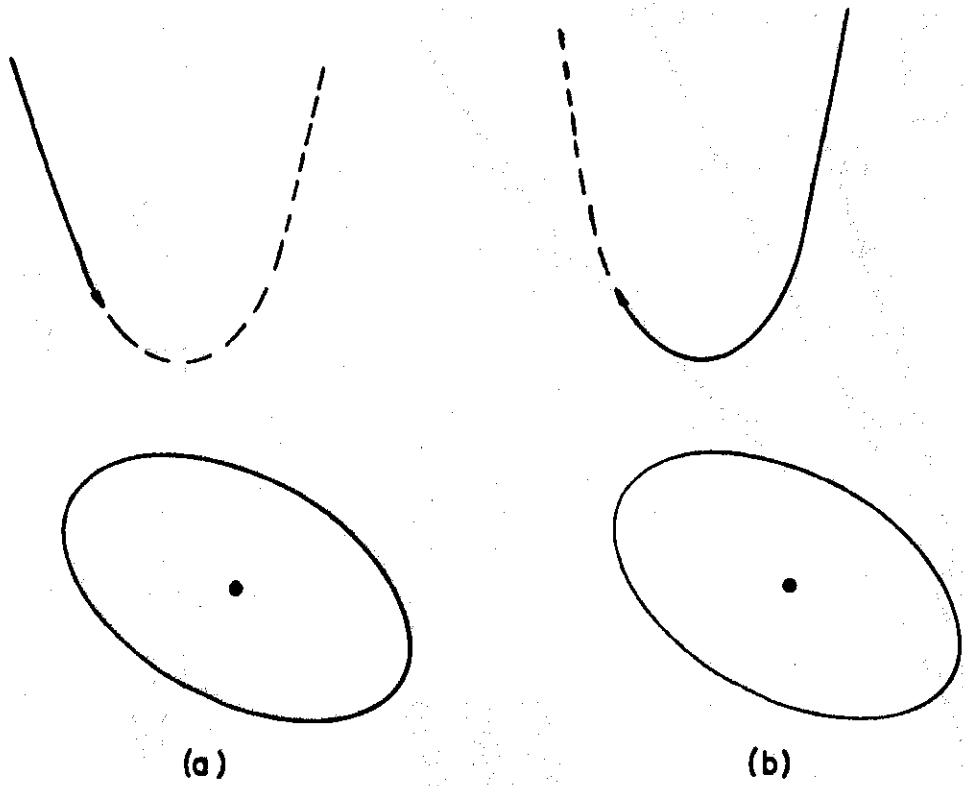


FIG. 4

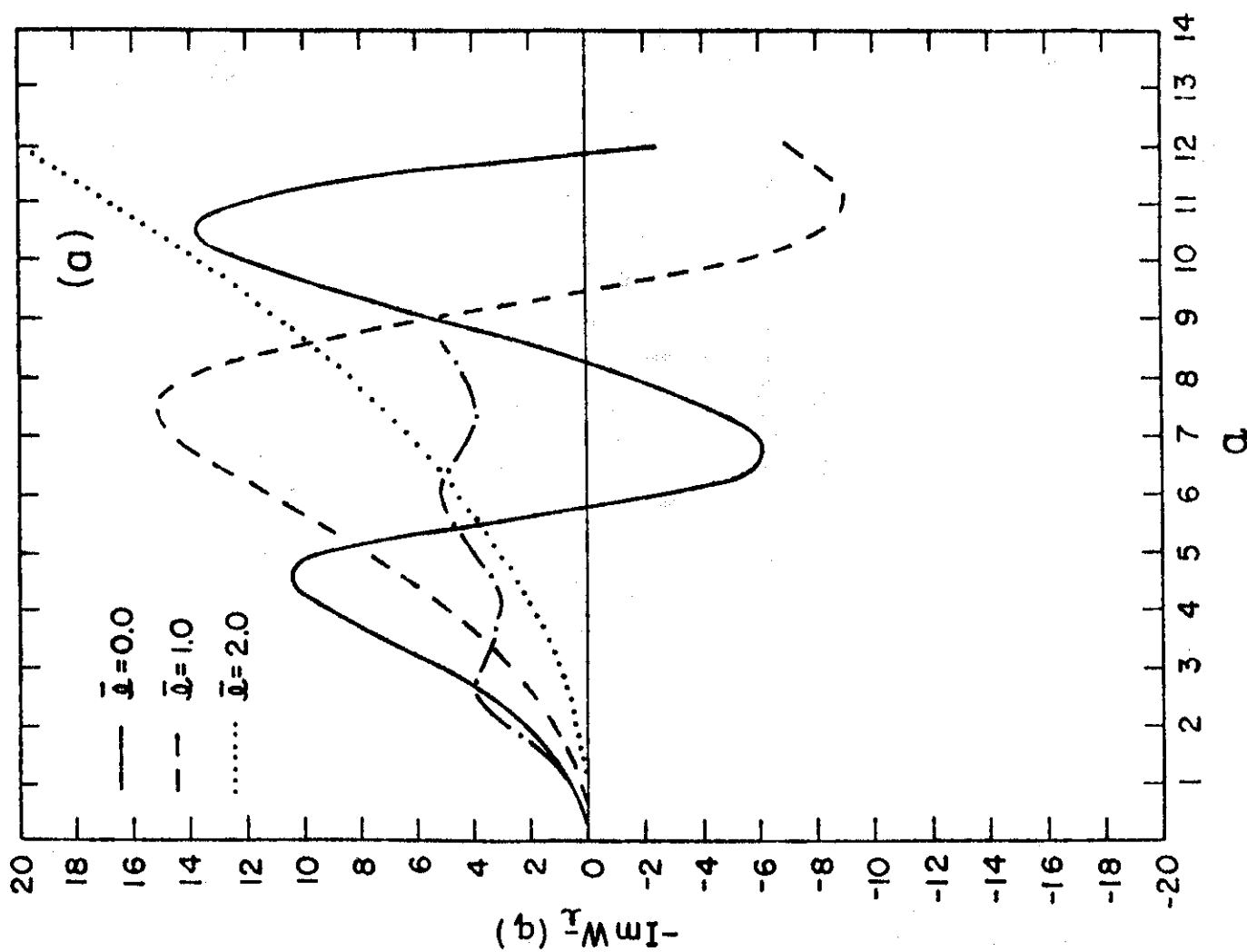
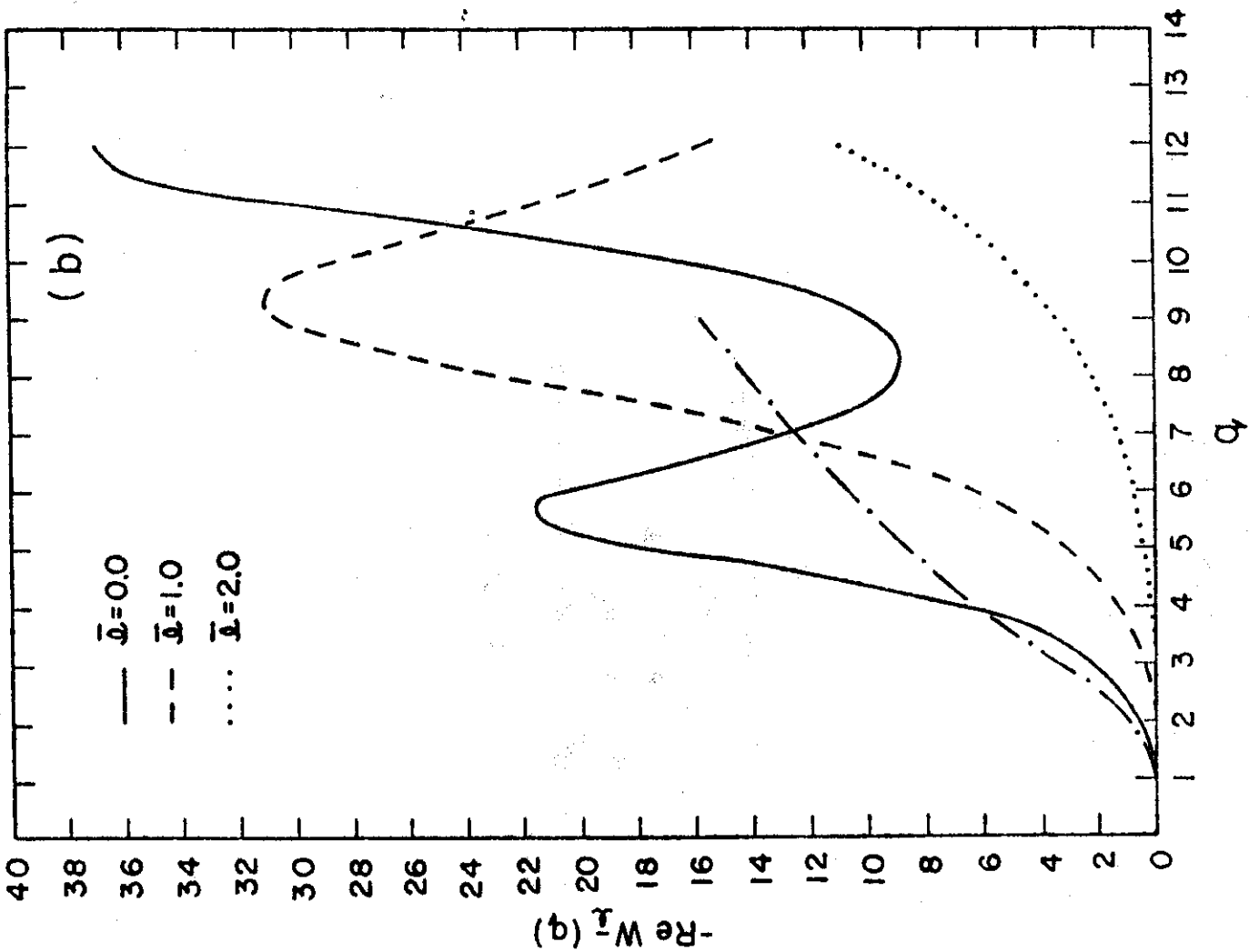


Figure 5

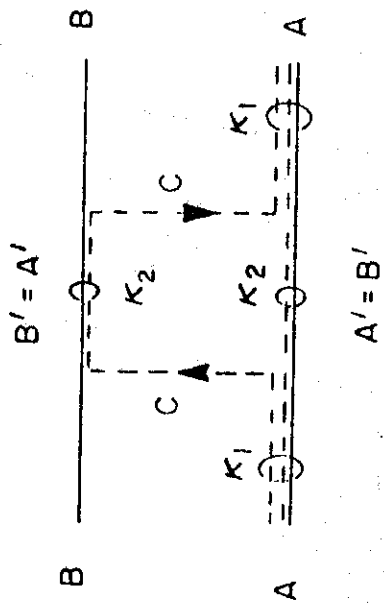
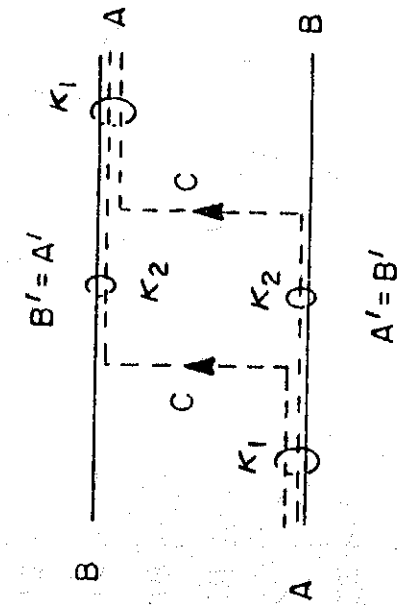


FIG. 6